International Journal of Engineering & Technology, 7 (4.13) (2018) 146-150

International Journal of Engineering & Technology

Website: www.sciencepubco.com/index.php/IJET

Research paper

Semi-infinite solid heat transfer limitation

Helmey Ramdhaney Mohd Saiah, Azmin Shakrine Mohd Rafie*, Fairuz Izzuddin Romli, Ahmad Salahuddin Mohd Harithuddin

Department of Aerospace Engineering, Faculty of Engineering, Universiti Putra Malaysia, 43400 Serdang, Selangor, Malaysia
**Corresponding author E-mail: shakrine@upm.edu.my*

Abstract

One-dimensional semi-infinite heat transfer solution is a common solution for transient heat transfer experiments. This solution is valid for a short certain amount of time before the semi-infinite solid became invalid. Crank Nicolson solution has been chosen to address this issue. This paper reports the time limitation for semi-infinite solid solution and justify the usability of Crank Nicolson solution given the same boundary conditions. The flat plate heat transfer experiment has been conducted. With the same boundary conditions, at Fourier number 0.1, the resultant heat transfer coefficient and adiabatic wall temperature have shown a good agreement between the semi-infinite solid solution and the Crank Nicolson solution. Beyond this Fourier number, both solutions have given inaccurate results. The inaccurate results are due to unsuitable boundary conditions. Future work will involve modification of the back face boundary conditions to address the time limitation of the one-dimensional semi-infinite solid heat transfer solution.

Keywords: *adiabatic wall temperature; Crank Nicolson solution; heat transfer coefficient; heat transfer solution.*

1. Introduction

In gas turbine cooling research, transient heat transfer experiments are very important. The resultant heat transfer parameters give the researchers a clear view of heat transfer processes involved. With these information, engineers could design engine components and cooling systems that are appropriate with the working temperature of the combustion chamber and turbine section. One of the most commonly used approaches to analyze the transient surface heat transfer experimental data is by solving Fourier one dimensional heat equation coupled with semi-infinite solid condition [1-6]. The resultant data would be heat transfer coefficient and adiabatic wall temperature.

Solving the Fourier one dimensional heat equation means that the heat is assumed to travel only in one direction. Furthermore, the semi-infinite solid condition supposes the subject to be infinitely long such that the heat does not thoroughly penetrate the subject. The semi-infinite solid condition will remain valid throughout the duration of the experiment as long as the back surface temperature does not change more than 1% of the wetted surface temperature [7]. The calculated heat transfer coefficient and also adiabatic wall temperature will be inaccurate if this semi-infinite solid condition is being violated. Most transient heat transfer cases require much longer experimental time to accurately calculate the heat transfer coefficient and adiabatic wall temperature [8]. The problem arises when the need for a longer experimental time violates the semi-infinite solid condition.

This paper aims to show the limitation of the semi-infinite solid solution by analyzing the experimental data beyond the allowable time limit. Crank Nicolson heat conduction solution is proposed to address this issue. However, before proceeding with this solution, its usability needs to be first verified. The content of this paper will include the justification on the Crank Nicolson solution with similar boundary conditions for the semi-infinite solid solution. The appropriate boundary conditions will be proposed at the end of this paper once the resultant heat transfer parameter from Crank Nicolson solution agrees well with the semi-infinite solid solution and the theoretical heat transfer coefficient. With similar boundary conditions, even though with different set of equations, the results should agree well with each other. Thus, hypothetically, the Crank Nicolson solution with the appropriate boundary conditions should allow the extension of the experimental time and also the accurate calculation the required heat transfer parameters.

2. Fourier one-dimensional heat transfer with semi-infinite solid condition

The surface temperature history data acquired from temperature sensors will usually be the main input for solving the Fourier one dimensional semi-infinite heat transfer condition. Unfortunately, in order to keep the semi-infinite solid condition to be valid, only partial of those surface temperature history data could be used to calculate heat transfer coefficient and adiabatic wall temperature. The Fourier equation for one dimensional heat conduction can be defined as in Eqn. 1.

$$\frac{\delta T}{\delta t} = \alpha \frac{\delta^2 T}{\delta x^2} \tag{1}$$

Assuming a solid with semi-infinite length exposed to step change in air temperature, the initial conditions can be set as follows:

$T = T_i$ for all x when $t = 0$
$T = T_i$ for all t as $x \rightarrow \infty$
Convection-conduction boundary condition at the wetted surface can be defined as;

$$q = -k\frac{\delta T}{\delta x} = h(T_{ad} - T_s) \text{at} x = 0 \text{ for } t > 0,$$

Copyright © 2018Authors. This is an open access article distributed under the Creative Commons Attribution License, which permits unrestricted use, distribution, and reproduction in any medium, provided the original work is properly cited.

in which T_i, T_{ad} and T_s are the initial, adiabatic wall and surface temperature respectively. The solution for Eqn. 1 can be written as;

$$\frac{T-T_i}{T_\infty-T_i} = erfc\left(\frac{x}{2\sqrt{\alpha t}}\right) - \exp\left(\frac{hx}{k}+\frac{h^2\alpha t}{k^2}\right)\left[erfc\left(\frac{x}{2\sqrt{\alpha t}}+\frac{h\sqrt{\alpha t}}{k}\right)\right] \quad (2)$$

T_∞ can also be defined as T_{ad}. Experimental time limit, t_L before the back surface temperature of insulation type material changes by 1% of the wetted surface temperature can be found in [7];

$$t_L = \frac{L^2}{9\alpha} \quad (3)$$

where L is the subject thickness and α is the thermal diffusivity of the subject's material. Figure 1 illustrates the condition for heat conduction in a semi-infinite solid.

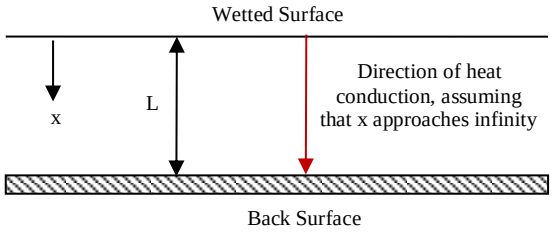


Fig. 1: Illustration of heat conduction in semi-infinite solid

If one were to choose polycarbonate with 15mm thickness as the test subject, according to Eqn. 3, the experimental time limit would be 188s before the back surface temperature changes more than 1% compared to the wetted surface temperature. The experimental time can also be represented by Fourier number, *Fo*;

$$Fo = \frac{\alpha t}{L^2} \quad (4)$$

where t is the experimental time. For a time limit of 188s, the corresponding *Fo* is 0.1. Solving Eqn. 2 for h = 60 W/m^{2}K, T_i = 15 °C and T_{ad} = 40 °C, and a polycarbonate thickness of 15 mm, the generated surface temperature history for about an hour of the experimental time, *Fo* = 2.0 can be represented by Figure 2.

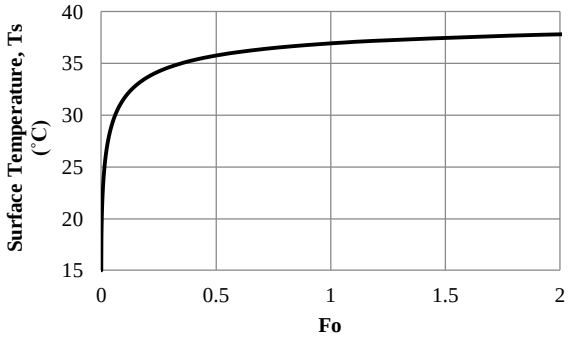


Fig. 2: Surface temperature history for 15 mm polycarbonate

It can be seen that even after an hour worth of experimental time, the theoretical surface temperature history would not reach the adiabatic wall temperature. In fact, in actual testing condition, only 3 minutes of experimental time are allowed in order to ensure that the semi-infinite solid condition is valid. Figure 3 shows the result if one were to use only 188s worth of surface temperature data to calculate the heat transfer coefficient and the adiabatic wall temperature.

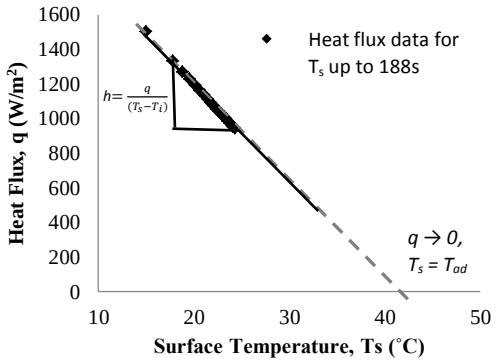


Fig. 3: Relationship between heat flux and surface temperature

The gradient of the graph in Figure 3 indicates the heat transfer coefficient, *h*. At *x* axis, when q = 0, the surface temperature correspond to the adiabatic wall temperature, $T_s = T_{ad}$. As shown in the figure by the dashed line, the result needs to be extrapolated to estimate the point at which the gradient of the graph intersect with *x* axis. This is to estimate the adiabatic wall temperature, T_{ad}. The lack of heat flux data at the lower portion of Figure 3 is due to the time limit for semi-infinite solid condition. Better result could be achieved if the experimental time can be extended. This will enable more surface temperature history data to be analyzed [8].

An alternative solution is proposed to address the limitation of the semi-infinite solid condition, which is based on finite difference method and Crank Nicolson one dimensional heat conduction. The convection-conduction wetted surface and the adiabatic back face boundary condition will be applied to the general Crank Nicolson solution to represent the semi-infinite solid solution condition. To verify this solution, the resultant heat transfer coefficient and the adiabatic wall temperature must be in agreement with the semi-infinite solid solution for *Fo* = 0.1, and most importantly, the theoretical heat transfer coefficient. The transient heat transfer experiment on a flat plate is chosen to provide the required surface temperature data. The experimental data will be analysed using semi-infinite solid solution and the Crank Nicolson solution with the same boundary conditions.

3. Heat transfer experiment

Earlier heat transfer experiments have utilized few methods such as bulky heaters [9] and preheated models [10, 11] to induce the step change in air temperature. A heating element, fast response stainless steel mesh heater, was invented to simplify the process of inducing hot air to the working environment [12]. This invention was chosen by majority of the researcher in their heat transfer experiments [13-15]. The current research work also utilizes the heating element for the heat transfer experiment.

A flat plate transient heat transfer experiment has been conducted to verify the Crank Nicolson solution with the semi-infinite solid solution. The experimental data will also be used to observe the effect of extended experimental time to the resultant heat transfer coefficient and the adiabatic wall temperature. The heat transfer experiment was conducted in a small wind tunnel utilizing the fast response mesh heater to induce the heat transfer process. The experiment was conducted for approximately half an hour, *Fo* = 0.95 at freestream air velocity of 27 m/s. Black coated, 15 mm polycarbonate flat plate was used as the test plate. Fast response thermocouple and infrared sensor were applied to measure the air temperature and surface temperature, respectively. The obtained experimental data were analysed separately for *Fo* = 0.1 and *Fo* = 0.95. Figure 4 shows the measured air temperature and surface temperature history data.

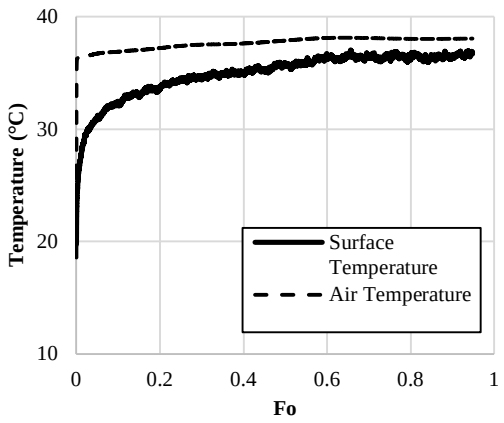


Fig. 4: Air temperature and surface temperature history

As mentioned earlier, the experimental data will be analysed using two methods, first is the two temperature solution method from [8] that uses the semi-infinite solid solution, and secondly by using Crank Nicolson finite difference method with adiabatic back face boundary condition.

4. Two temperature solution method

Eqn. 2 can be written in non-dimensional form as;

$$\theta = erfc\left(\frac{x}{2\sqrt{Fo}}\right) - \exp(xBi + Bi^2 Fo)\left[erfc\left(\frac{x}{2\sqrt{Fo}} + BiFo^{1/2}\right)\right] \quad (5)$$

where;

$$\theta = \frac{T - T_i}{T_{ad} - T_i} \quad (6)$$

$$Bi = \frac{hL}{k} \quad (7)$$

At the wetted surface, where x = 0, Eq. (5) can be reduced to;

$$\theta_s = 1 - \exp(Bi^2 Fo)erfc\left(BiFo^{1/2}\right) \quad (8)$$

Substituting;

$$X = BiFo^{1/2} \quad (9)$$

Eq. (8) becomes;

$$\theta_s = 1 - \exp(X^2)erfc(X) \quad (10)$$

For the two temperature method solution, two temperature data will be taken from the surface temperature history data, denoted by;

$$\theta_1 = 1 - \exp({X_1}^2)erfc(X_1) \quad (11)$$

$$\theta_2 = 1 - \exp\left({X_2}^2\right)erfc(X_2) \quad (12)$$

Dividing Eq. (11) to Eq. (12) yield;

$$\frac{\theta_1}{\theta_2} = \frac{1 - \exp({X_1}^2)erfc(X_1)}{1 - \exp({X_2}^2)erfc(X_2)} \quad (13)$$

Eq. (9) can also be defined as;

$$X = BiFo^{1/2} = h\left[\frac{t}{\rho c_p k}\right]^{\frac{1}{2}} \quad (14)$$

Expression for X_1 and X_2 becomes;

$$X_1 = h\left[\frac{t_1}{\rho c_p k}\right]^{\frac{1}{2}} \quad (15)$$

$$X_2 = h\left[\frac{t_2}{\rho c_p k}\right]^{\frac{1}{2}} \quad (16)$$

Dividing Eqn. 15 to Eqn. 16 yields;

$$\frac{X_1}{X_2} = \left[\frac{t_1}{t_2}\right]^{\frac{1}{2}} \quad (17)$$

Therefore, X_1 can be expressed in terms of X_2;

$$X_1 = X_2\left[\frac{t_1}{t_2}\right]^{\frac{1}{2}} \quad (18)$$

Eqn. 10 can be also rearranged as;

$$f(X) = \theta_s - 1 + \exp(X^2)erfc(X) \quad (19)$$

so that Eqn. 13 becomes;

$$f(X) = \frac{\theta_1}{\theta_2} - \frac{1 - \exp({X_1}^2)erfc(X_1)}{1 - \exp({X_2}^2)erfc(X_2)} \quad (20)$$

Substituting X_1 into Eqn. 20 yields;

$$f(X_2) = \frac{\theta_1}{\theta_2} - \frac{1 - \exp\left(\frac{t_1}{t_2}{X_2}^2\right)erfc(\left[\frac{t_1}{t_2}\right]^{\frac{1}{2}}X_2)}{1 - \exp\left({X_2}^2\right)erfc(X_2)} \quad (21)$$

Introducing f_1 and f_2 to simplify the Eqn. 21;

$$f_1 = 1 - \exp\left(\frac{t_1}{t_2}{X_2}^2\right)erfc(\left[\frac{t_1}{t_2}\right]^{\frac{1}{2}}X_2) \quad (22)$$

$$f_2 = 1 - \exp\left({X_2}^2\right)erfc(X_2) \quad (23)$$

Hence Eqn. 21 becomes;

$$f(X_2) = \frac{\theta_1}{\theta_2} - \frac{f_1}{f_2} \quad (24)$$

Yan and Owen [4] suggested to use the value of θ_2 as large as possible with θ_1 half the value of θ_2. Taking that into consideration and picking out two temperature data from the surface temperature history, heat transfer coefficient and adiabatic wall temperature are determined. Newton Raphson iteration can be used to find X_2 value, and subsequently X_1 in Eqn. 18, θ_1 in Eqn. 11, θ_2 in Eqn. 12, h in Eqn. 14 and T_{ad} in Eqn. 6.

$$X_{2,n+1} = X_{2,n} - \frac{f(X_{2,n})}{f'(X_{2,n})} \quad (25)$$

with;

$$f'(X_{2,n}) = \frac{\left[1 - \exp({X_2}^2)erfc(X_2)\right]\left[2\left(\begin{array}{c}\frac{\left(\frac{t_1}{t_2}\right)^{\frac{1}{2}}}{\sqrt{\pi}} - \left(\frac{t_1}{t_2}\right)X_2\left(\exp\left(\frac{t_1}{t_2}\right)X_2^2\right) \\ \left(erfc\left(\frac{t_1}{t_2}\right)^{\frac{1}{2}}X_2\right)\end{array}\right)\right] - \left[1 - \exp\left(\left(\frac{t_1}{t_2}\right)X_2^2\right)erfc\left(\frac{t_1}{t_2}\right)^{\frac{1}{2}}X_2\right]\left[2\left(\frac{1}{\sqrt{\pi}} - X_2\left(\exp({X_2}^2)\right)(erfc(X_2))\right)\right]}{\left[1 - \exp({X_2}^2)erfc(X_2)\right]^2} \quad (26)$$

Table 1 summarizes the result from the two temperature solution method. The air temperature is measured by the fast response thermocouple and a theoretical flat plate heat transfer coefficient is used as the reference. The theoretical flat plate heat transfer coefficient can be taken from [16] by using freestream velocity of 27 m/s,

$$h = 0.0296Re^{-\frac{1}{5}}Pr^{-\frac{2}{3}}\rho c_p U \quad (27)$$

Table 1: Comparison between *Fo* = 0.1 and 0.9 for two temperature solution method

Fo	Exp. time (s)	Theoretical h (W/m^{2}K)	Air temp. (°C)	h (W/m^{2}K)	T_{ad} (°C)
0.1	188	89.2	36.9	95.5	36.2
0.95	1600		38.5	74.5	38.5

In Table 1, for *Fo* = 0.1, the resultant heat transfer coefficient is overestimated by 7% while the adiabatic wall temperature is underestimated by 2%. For *Fo* = 0.95, a considerably longer experimental time results in an underestimated heat transfer coefficient by 16%. The adiabatic wall temperature agrees well with the measured air temperature. The increased error in heat transfer coefficient for longer experimental time is to be expected. This reason for this increase will be made clear when the experimental data is analysed using the Crank Nicolson solution.

5. Crank Nicolson heat conduction solution

The general Crank Nicolson solution for heat conduction can be written as;

$$(-Fo)T_{i-1}^{n+1} + (2+2Fo)T_{i1}^{n+1} + (-Fo)T_{i+1}^{n+1} = (Fo)T_{i-1}^{n} + (2-2Fo)T_{i}^{n} + (Fo)T_{i+1}^{n} \quad (28)$$

With Fourier number, $Fo = \frac{\alpha t}{L^2} = \frac{\alpha \Delta t}{(\Delta x)^2}$, for the wetted surface with convection-conduction boundary condition;

$$q = h(T_{air} - T_i) = \frac{k}{\Delta x}(T_i - T_{i+1}) \quad (29)$$

The Eqn. 28 can be rearranged to;

$$(2BiFo + 2 + 2Fo)T_i^{n+1} + (-2Fo)T_{i+1}^{n+1} + (-2BiFo)T_{air} = (-2BiFo + 2 - 2Fo)T_i^n + (2Fo)T_{i+1}^n + (2BiFo)T_{air} \quad (30)$$

For adiabatic back face boundary condition,

$$q = \frac{k}{\Delta x}(T_i - T_{i+1}) = h(T_i - T_{amb}) \quad (31)$$

With h = 0 at the back face indicating adiabatic condition, and i = L, Eqn. 28 can be rearranged to;

$$(-Fo)T_{L-1}^{n+1} + (1+Fo)T_L^{n+1} = FoT_{L-1}^n + (1-Fo)Ti_L^n \quad (32)$$

The experimental data can be analysed numerically by using Eqn. 30 for the wetted surface, Eqn. 28 for internal nodes and Eqn. 32 for the back face condition. Figure 5 and Figure 6 represent the heat flux data for *Fo* = 0.1 and 0.95, respectively.

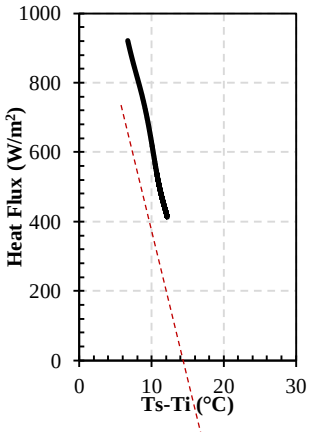


Fig. 5: Heat flux data for *Fo* = 0.1

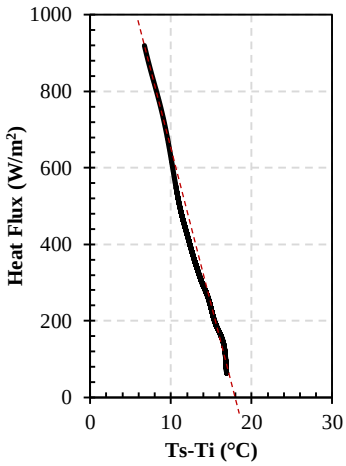


Fig. 6: Heat flux data for *Fo* = 0.95

The gradient of the red dotted line in both figures indicates the heat transfer coefficient value. The point where the red dotted line intersect with x-axis indicates the adiabatic wall temperature. It can be seen that a longer experimental time allows more surface temperature data to be analysed for determination of heat transfer coefficient and adiabatic wall temperature. However, solely by just be having more data to be analysed does not guarantee an increased accuracy or reliability. Additional surface temperature history data must be analysed using another set of the boundary condition to fit the experimental conditions. The adiabatic back face boundary condition must be replaced with a more appropriate boundary condition. Table 2 summarizes the resultant heat transfer coefficient and the adiabatic wall temperature for Crank Nicolson solution.

Table 2: Comparison between *Fo* = 0.1 and 0.9 for Crank Nicolson numerical solution

Fo	Exp. time (s)	Theoretical h (W/m^{2}K)	Air temp. (°C)	h (W/m^{2}K)	T_{ad} (°C)
0.1	188	89.2	36.9	95.6	36.1
0.95	1600		38.5	61.9	38.4

In Table 2, for *Fo* = 0.1, the resultant heat transfer coefficient is overestimated by 7% while the adiabatic wall temperature is underestimated by 2%. This difference agrees well with the two temperature solution method that uses the semi-infinite solid solution. These results justify the usability of the Crank Nicolson solution for *Fo* = 0.1, with convection-conduction wetted surface and adiabatic back face boundary condition. For *Fo* = 0.95, the heat transfer coefficient is underestimated by 30%. This is much worst compared to the 16% for the two temperature solution method. This incorrect value is to be expected due to the boundary conditions applied to the Crank Nicolson solution. The adiabatic wall temperature however agrees well with the measured air temperature with only 0.2% difference.

The results using this boundary conditions can only be used for *Fo* = 0.1. For *Fo*> 0.1, it does not matter if one uses the semi-infinite solid solution or the Crank Nicolson (convection-conduction wetted surface, adiabatic back face) solution, the results will always be incorrect. Therefore, if the back face boundary condition of the Crank Nicolson solution can be changed to conduction-convection condition, hypothetically, this will enable for a longer experimental time. This paper involves only a set of transient heat transfer experimental data at 27 m/s of freestream air velocity. Series of transient heat transfer experiments at a range of freestream air velocity can be found in [17]. The paper also includes the plotted resultant heat transfer coefficient from Crank Nicolson solution with adiabatic back face to the theoretical flat plate heat transfer correlation.

6. Conclusion

The limitation for the existing one-dimensional heat transfer with semi-infinite solid condition solution was pointed out. Due to the time restriction of semi-infinite solid condition, the resultant heat transfer coefficient and adiabatic wall temperature can only stay valid for a short period of experimental time, $Fo \leq 0.1$. The Crank Nicolson finite difference solution was chosen as an alternative solution. Heat transfer coefficient and adiabatic wall temperature for the semi-infinite solution and the Crank Nicolson solution are compared. For $Fo = 0.1$, both results agree well with the theoretical values. This indicates that with the same boundary conditions as the semi-infinite solution, the Crank Nicolson solution proves to be reliable. However, the results for longer experimental time, $Fo = 0.95$ do not agree with the theoretical value. This proves a good point because the boundary conditions used for both solutions are not meant for $Fo > 0.1$. For $Fo > 0.1$, the semi-infinite solution could not be used and the Crank Nicolson solution with adiabatic back face needs to be changed to conduction-convection condition. It is expected that, in future work, modification to the back face boundary condition will result in a more reliable data. This will help researchers to set a longer experimental time for heat transfer experiments.

7. Future work

The next step is to modify boundary conditions of the Crank Nicolson solution. The boundary condition on the wetted surface will be the same, while the back face will have a conduction-convection boundary condition. With another set of back surface boundary condition, hypothetically, it will allow the experimental time to be extended to a longer time. Longer experimental time will allow more surface temperature data to be used for analysis. Ultimately, these additional surface temperature data will result in a more reliable and accurate heat transfer coefficient and adiabatic wall temperature.

Acknowledgement

The authors acknowledge the funding for this research by the Ministry of Education Malaysia and Universiti Putra Malaysia, Putra Grant No. 9531600. The authors also thank supervisors from University of Bath for their guidance in this study.

Nomenclature

Bi	Biot number [hL/k_{solid}]
c_p	Specific heat
F	Function in semi-infinite solution
f	Parameter in semi-infinite solution
Fo	Fourier number [$\alpha t/L^2$]
h	Heat transfer coefficient
k	Thermal conductivity
L	Characteristic length, total thickness
q	Heat flux
Re	Reynolds number [$\rho Ux/\mu$]
Pr	Prandtl number
t	time
T	Temperature
T_{ad}	Adiabatic wall temperature
T_i	Initial temperature
T_s	Surface temperature
U	Velocity
x	Distance
X	Parameter in semi-infinite solution

Greek symbols

α	Thermal diffusivity [$k/\rho c_p$]
μ	Dynamic viscosity
ρ	Density
∞	Freestream, Infinity
θ	Non-dimensional temperature [$(T - T_i)/(T_{ad} - T_i)$]
θ_s	Non-dimensional surface temperature [$(T_s - T_i)/(T_{ad} - T_i)$]
θ_1	Non-dimensional temperature for crystal 1 [$(T_{s1} - T_i)/(T_{ad} - T_i)$]
θ_2	Non-dimensional temperature for crystal 2 [$(T_{s2} - T_i)/(T_{ad} - T_i)$]

References

[1] Baughn JW (1995), Liquid crystal methods for studying turbulent heat transfer. *Int. J. Heat and Fluid Flow* 16, 365-375

[2] Chambers AC, Gillespie DRH, Ireland PT & Dailey GM (2003), A novel transient liquid crystal technique to determine heat transfer coefficient distributions and adiabatic wall temperature in a three-temperature problem. *Journal of Turbomachinery* 125, 538-546

[3] Ireland PT & Jones TV (2000), Liquid crystal measurements of heat transfer and surface shear stress. *Meas. Sci. Technol.* 11, 969-986

[4] Yan Y & Owen JM (2002), Uncertainties in transient heat transfer measurements with liquid crystal. *International Journal of Heat and Fluid Flow* 23, 29-35

[5] Abu Talib AR, Jaafar AA, Mokhtar AS, Mohd Saiah HR, Abd. Rahim I & Abdul Karim MS (2006), Effects of blowing ratio on the heat transfer coefficient distribution downstream of a single film cooling hole. *International Journal of Engineering and Technology* 3(1), 37-46

[6] Ramli MS, Abu Talib AR, Harmin MY & Mohd Saiah HR (2016), Effect of multiple jet impingement plate configurations on Reynolds number in a pipe. *IOP Conf. Series: Materials Science and Engineering* 152

[7] Shultz DL & Jones TV (1973), Heat transfer measurement in short duration hypersonic facilities. Advisory Group for Aerospace Research and Development, Paris, France

[8] Pountney O, Cho GH, Lock GD & Owen JM (2012), Solutions of Fourier's equation appropriate for experiment using thermochromic liquid crystal. *International Journal of Heat and Mass Transfer* 55, 5908-5915

[9] Clifford RJ, Jones TV & Dunne ST (1983), Techniques for obtaining detailed heat transfer coefficient measurements within gas turbine blade and vane cooling passages. ASME International Gas Turbine Conference and Exhibit

[10] O'Brien JE, Simoneau RJ, LaGraff JE & Morehouse KA (1986), Unsteady heat transfer and direct comparison for steady state measurements in a rotor wake experiment. International Heat Transfer Conference

[11] Hippensteele SA & Russell LM (1988), High-resolution liquid-crystal heat transfer measurements on the endwall of a turbine passage with variations in Reynolds number. ASME National Heat Transfer Conference

[12] Ireland PT, Gillespie DRH & Wang Z (1996), Heating Element. WIPO, *World Intellectual Property Organization*, Patent No: GB9602017

[13] Ireland PT, Neely AJ, Gillespie DRH & Robertson AJ (1999), Turbulent heat transfer measurements using liquid crystals. *International Journal of Heat and Fluid Flow* 20, 355-367

[14] Son C, Gillespie D, Ireland P & Dailey GM (2001), Heat transfer and flow characteristics of an engine representative impingement cooling system. *Journal of Turbomachinery* 123, 154-160

[15] Mohd Saiah HR, Abu Talib AR, Abdullah N, Abdul Jalil NA & Mokhtar AS (2008), Experimental investigation of fast response heater for transient heat transfer application, HFT_0041

[16] Holman JP (2010), *Heat Transfer*. McGraw-Hill Higher Education

[17] Mohd Saiah HR, Mohd Rafie AS & Romli FI (2018), Freestream velocity correction in narrow channels. *Journal of Mechanical Engineering* SI5(2), 54-66